Journal of Biomolecular Screening
http://jbx.sagepub.com/

Development of a Novel High-Throughput Screen and Identification of Small-Molecule Inhibitors of the Gα–RGS17 Protein–Protein Interaction Using AlphaScreen

Duncan I. Mackie and David L. Roman

J Biomol Screen 2011 16: 869 originally published online 16 June 2011
DOI: 10.1177/1087057111410427

The online version of this article can be found at:
http://jbx.sagepub.com/content/16/8/869

Published by:
SAGE
http://www.sagepublications.com

Additional services and information for *Journal of Biomolecular Screening* can be found at:

Email Alerts: http://jbx.sagepub.com/cgi/alerts

Subscriptions: http://jbx.sagepub.com/subscriptions

Reprints: http://www.sagepub.com/journalsReprints.nav

Permissions: http://www.sagepub.com/journalsPermissions.nav

>> Version of Record - Sep 9, 2011

Proof - Jun 16, 2011

What is This?

Downloaded from jbx.sagepub.com at Novartis Global on October 21, 2011

Development of a Novel High-Throughput Screen and Identification of Small-Molecule Inhibitors of the Gα–RGS17 Protein–Protein Interaction Using AlphaScreen

DUNCAN I. MACKIE[1] and DAVID L. ROMAN[1,2]

In this study, the authors used AlphaScreen technology to develop a high-throughput screening method for interrogating small-molecule libraries for inhibitors of the $G\alpha_o$–RGS17 interaction. RGS17 is implicated in the growth, proliferation, metastasis, and the migration of prostate and lung cancers. RGS17 is upregulated in lung and prostate tumors up to a 13-fold increase over patient-matched normal tissues. Studies show RGS17 knockdown inhibits colony formation and decreases tumorigenesis in nude mice. The screen in this study uses a measurement of the $G\alpha_o$–RGS17 protein–protein interaction, with an excellent Z score exceeding 0.73, a signal-to-noise ratio >70, and a screening time of 1100 compounds per hour. The authors screened the NCI Diversity Set II and determined 35 initial hits, of which 16 were confirmed after screening against controls. The 16 compounds exhibited IC_{50} <10 μM in dose–response experiments. Four exhibited IC_{50} values <6 μM while inhibiting the $G\alpha_o$–RGS17 interaction >50% when compared to a biotinylated glutathione-S-transferase control. This report describes the first high-throughput screen for RGS17 inhibitors, as well as a novel paradigm adaptable to many other RGS proteins, which are emerging as attractive drug targets for modulating G-protein-coupled receptor signaling. (*Journal of Biomolecular Screening* 2011;16:869-877)

Key words: RGS protein, G protein, high-throughput screening, AlphaScreen, protein–protein interactions

INTRODUCTION

THE LARGEST KNOWN FAMILY OF CELL SURFACE RECEPTORS is the G-protein-coupled receptors (GPCRs).[1] These heptahelical plasma membrane–spanning receptors transduce signals initiated by extracellular stimuli such as hormones and light by coupling to intracellular G-proteins. G-proteins are heterotrimers consisting of α and βγ subunits. α subunits are grouped into subfamilies comprising $G\alpha_{o/i,}$ $G\alpha_s$, $G\alpha_q$, $G\alpha_{12/13}$, $G\alpha_{olf}$, and $G\alpha_z$. GPCRs have become the target of more than 50% of current therapeutic agents on the market and are thus the subject of great research interest.[2] Mechanistically, GPCRs are activated upon agonist binding and, through conformational changes, affect an exchange of guanosine diphosphate (GDP) for guanosine triphosphate (GTP) on Gα, which causes dissociation of the heterotrimer into α and βγ subunits.[3] $G\alpha_o$ subunits exhibit slow intrinsic GTPase activity, which inactivates the G-protein when GTP is hydrolyzed and returns the α subunit to its inactive GDP-bound form. Once inactive, the α subunit reassociates with the βγ subunit and reforms the heterotrimer, which can reassociate with GPCRs. Modulation of inhibitory Gα subunit signaling activity, such as that mediated by $G\alpha_{i/o}$, occurs by regulator of G-protein signaling (RGS) proteins. RGS proteins are GTPase activating proteins (GAPs) and accelerate the slow intrinsic GTPase activity of Gα subunits by binding to the active, GTP-bound form of Gα and facilitating more rapid exchange of GDP for GTP. RGS proteins are not directly responsible for hydrolysis of GTP but instead cause structural changes in the active Gα–GTP complex, which results in a more favorable conformation of the complex for efficient hydrolysis of GTP.[4–6]

Structurally, RGS proteins are hallmarked by the RGS homology (RH) domain that defines them as GAPs.[6] The mammalian family of RGS proteins contains more than 30 members, all of which possess the ca. 120 amino acid RH domain.[5,7] RGS proteins are divided into eight subfamilies according to the shared sequence identities found outside of the RH domain.[5,6] Members of the A/RZ and B/R4 subfamilies are the smallest RGS proteins and consist of the RH domain flanked by small but variable N- and C-terminal regions.[5–7] Members of the other

[1]Division of Medicinal and Natural Products Chemistry, College of Pharmacy, University of Iowa, Iowa City, IA.
[2]The Holden Comprehensive Cancer Center, University of Iowa Hospitals and Clinics, Iowa City, IA.

Received Dec 23, 2010, and in revised form Mar 17, 2011. Accepted for publication Mar 18, 2011.

Supplementary material for this article is available on the *Journal of Biomolecular* Screening Web site at http://jbx.sagepub.com/supplemental.

Journal of Biomolecular Screening 16(8); 2011
DOI: 10.1177/1087057111410427

© 2011 Society for Laboratory Automation and Screening

Downloaded from jbx.sagepub.com at Novartis Global on October 21, 2011

six families are multidomain proteins that vary in size and function within the cell.

One in 4 deaths in the United States is due to cancers. The *Cancer Journal for Clinicians* projects more than 1.5 million new cancer diagnoses and more than 550 000 deaths from cancer in the United States in 2010.[8] A growing number of studies have implicated the overexpression of RGS proteins playing a role in the progression of cancer. Some examples include the overexpression of RGS1 in melanoma and ovarian cancer[9,10]; RGS2 in breast cancer[11]; RGS5 in melanoma, multiple myeloma, acute myeloid leukemia, and ovarian and breast cancer[12]; RGS19 in ovarian cancer[13]; RGS20 in melanoma[14]; and RGS17 in lung and prostate cancers.[15,16] These RGS proteins present a unique target for advances in cancer drug discovery leading to new avenues for anticancer therapies and treatment options for patients diagnosed with cancer.

Our lab has an interest in the role of RGS proteins in lung and prostate cancer. In this report, we focus on RGS17. RGS17 is a member of the A/RZ subfamily of RGS proteins and contains the RH domain and an N-terminal cysteine string domain.[6] RGS17 is normally expressed in the human central nervous system with the highest levels of mRNA expressed in the cerebellum, nucleus accumbens, and putamen.[17] RGS17 regulates $G\alpha_{i/o}$, $G\alpha_z$, and $G\alpha_q$ and accelerates the rate of GTPase activity by these alpha subunits.[18] The $G\alpha_{i/o}$ and $G\alpha_z$ subunits inhibit adenylate cyclase and downregulate cAMP formation, which attenuates the cAMP-PKA-CREB signaling cascade. PKA is a holoenzyme that is assembled as an inactive tetrameric complex consisting of two regulatory subunits (R-PKA) and two catalytic subunits (C-PKA).[19–21] In response to the elevated cAMP levels in the cell, the C-PKA subunits move into the nucleus where they phosphorylate the transcription factor, cyclic AMP response element (CRE)–binding protein (CREB).[22–24] Once CREB is phosphorylated, transcription of more than 4000 genes begins.[22,25] Recently, it has been reported that CREB is involved in the development and tumorigenesis of endocrine tissues and lung adenocarcinoma.[26,27] Normal levels of RGS17 serve to modulate the cAMP-PKA-CREB signaling cascade, but in lung cancers, RGS17 transcripts are increased in 80% of tumors by an average of 8.3-fold over patient-matched normal lung tissues.[15] Transcript accumulation also occurs in prostate tumors by an average of 7.5-fold when compared to patient-matched normal tissue samples.[15] The increase in RGS17 acts to attenuate $G\alpha_{i/o}$ and $G\alpha_z$ signaling, which results in increased cAMP in tumor cells, which activates the cAMP–PKA–CREB pathway that induces tumor cell proliferation and tumorigenesis.[15,16] Recent RNAi knockdown studies involving H1299 cells have shown that cell proliferation, measured by MTT assays, can be attenuated when RGS17 levels are decreased.[15,16] RGS17 knockdown in HCT116 and H1299 cells exhibited slow growth and decreased tumor size in nude mice tumorigenesis assays.[15,16]

The goal of this study was to develop and implement a high-throughput screening (HTS) assay to identify small molecules that inhibit the $G\alpha_o$–RGS17 protein–protein interaction, using AlphaScreen technology (PerkinElmer, Waltham, MA). AlphaScreen has been previously used to screen for numerous antagonists of protein–protein interactions, including STAT–SH2[28] and Hsp90–cochaperone.[29] In this study, we report the first use of AlphaScreen for RGS protein interactions. Previous HTS efforts using different methods, such as the flow cytometry protein interaction assay (FCPIA), have been used to identify inhibitors for RGS4.[30–32] This method was formatted in 96-well plates and involved screening approximately 160 compounds per hour. Our goal for developing a new HTS assay was to increase the amount of compounds screened to more than 1000 compounds/hour while maintaining a robust Z factor with an excellent signal-to-noise ratio as seen in FCPIA.

Using AlphaScreen, we established a pilot screen in which we screened 1364 compounds from the National Cancer Institute (NCI) Diversity Set II to identify inhibitors of the $G\alpha_o$–RGS17 protein–protein interaction in preparation for screening large libraries as part of our research program. This pilot screen resulted in four putative RGS17 inhibitors, all of which exhibited IC_{50} values less than 6 μM. Here we report the development and describe the evolution of bead-based HTS for RGS protein interactions into a faster and more robust assay, as well as the first HTS paradigm for RGS17 inhibitors focused on anticancer lead development.

MATERIALS AND METHODS

RGS protein expression and purification

Human RGS17 in the pcDNA3.1 (+) vector was purchased from the Missouri S&T cDNA Resource Center (Rolla, MO; www.cdna.org). The RGS17 open reading frame was amplified using the following primers: 5′-GGGGA CAAGTTTGTACAA AA AAGCAGGCTTA ATGGAGAGTATCCAGGTC-3′ and 5′-GG GGACCACTTTGTACAAGAAAGCTGGGTAA GATT CAGA AGAAGAGCC-3′. This also created an attB-flanked PCR product compatible with Gateway (Invitrogen, Irvine CA) cloning. The attB-flanked PCR product was combined with the donor vector pDONR221, using Gateway technology with Clonase II (Invitrogen, Carlsbad, CA) according to manufacturer's protocols. The Gateway technology uses the lambda recombination system to facilitate transfer of heterologous DNA sequences flanked by modified att sites between vectors. The resulting pDONR221/RGS17 vector was transformed into DH5-α bacteria, colonies were picked, and DNA was mini-prepped (Qiagen, Valencia, CA). The donor vector containing RGS17 was combined with the expression vector pDEST565 (Addgene plasmid 11520, Dominic Esposito, SAIC-Frederick) in LR recombination reaction (Invitrogen) according to the manufacturer's instructions. This produced RGS17 with an N-terminal glutathione-S-transferase (GST) and a C-terminal 6xHis tag. RGS17/pDEST565 was transformed into BL-21 (DE3) bacteria,

Downloaded from jbx.sagepub.com at Novartis Global on October 21, 2011

and a single colony was picked and expanded into a 2-L culture of LB containing 100 μg/mL ampicillin and induced at OD600 = 0.6 with 500 μM isopropyl β-D-1-thiogalactopyranoside (IPTG) for 4 h at 37 °C. Bacteria were pelleted and resuspended in RGS17 buffer (50 mM HEPES [pH 7.4], 100 mM NaCl, 2 mM $MgCl_2$, 1 mM β-mercaptoethanol, 0.1% Triton X-100) with added protease inhibitors (final concentrations: 1 μM E-64, 1 mM phenylmethanesulfonylfluoride [PMSF], 1 μM leupeptin, and 1 μM pepstatin A) and treated with 0.5 mg/mL lysozyme for 15 min while stirring on ice. The suspension was flash-frozen in liquid nitrogen and thawed. Following lysis, DNAse I was added while stirring on ice. The lysate was centrifuged for 45 min at 36 500 rpm (~100 000 *g*) in a Sorvall T-647.5 rotor. The supernatant was filtered (0.45 μm) and applied to a 5-mL nickel-NTA agarose column (Qiagen). The resin was washed with 15 mL RGS17 buffer containing 40 mM imidazole. Protein was eluted with RGS17 buffer containing 200 mM imidazole in 1.5-mL fractions. Following sodium dodecyl sulfate polyacrylamide gel electrophoresis (SDS-PAGE) analysis, RGS17 fractions were pooled and diluted with RGS17 buffer to 50 mM imidazole concentration and incubated with 3 mL GST resin (Qiagen) for 3 h at 4 °C on an inversion mixer. RGS17 was eluted using a batch method with 10 mM reduced glutathione and taking 10 × 1-mL fractions. This procedure resulted in ~95% pure RGS17 (20 mg at 1.2 mg/mL).

$G\alpha_o$ protein expression and purification

6x-His-tagged $G\alpha_o$ was expressed and purified from transformed BL-21 (DE3) bacteria as described previously[33] with the exception of 1 mM Tris(2-carboxyethyl)phosphine hydrochloride (TCEP) in the buffer in place of 1 mM dithiothreitol (DTT) as the reducing agent.

Chemical biotinylation of $G\alpha_o$ protein

$G\alpha_o$ proteins were biotinlyated with 1-biotinamido-4-[4′-(maleimidomethyl)cyclohexanecarboxamido] butane (533.68 g/mol) using EZ-Link Biotin-BMCC (Thermo Scientific, Rockford, IL). Protein was labeled at a 10:1 biotin/protein ratio following manufacturer protocols. Excess biotin was removed by applying the sample to an 8-mL fast-flow desalting fast protein liquid chromatography (FPLC) column running at 1 mL/min on an AKTA (GE Healthcare, Piscataway, NJ) purifier system. Fractions were pooled and concentrated to 1.66 mg/mL using an Ultracel 10K centrifugal filter (Millipore, Billerica, MA) and snap-frozen in liquid nitrogen.

DMSO tolerance test

AlphaScreen beads were provided by PerkinElmer in a suspension of 5 mg/mL. Four sets of 10 wells were used to determine the tolerance of the assay to an upper limit of 3.3% DMSO, which represents the maximum theoretical concentration of DMSO in planned follow-up dose–response experiments, and a concentration in excess of our screening concentration of <1.5%. Then, 24.4 μg (4.88 μL) of anti-GST acceptor beads was incubated with GST–RGS17 at a 30nM concentration in 200 μL of assay buffer (50 mM HEPES, 100mM NaCl, 0.1% Lubrol, 1% bovine serum albumin [BSA], pH 8.0) for 30 min at room temperature while streptavidin donor beads (PerkinElmer) were incubated with biotin–$G\alpha_o$ at a 30nM concentration in 200 μL assay buffer. Following the coupling incubation, RGS17–anti-GST beads were brought to a final volume of 610 μL with assay buffer. $G\alpha_o$–biotin–streptavidin beads were split into two equal aliquots designated + or – AMF (50 mM NaF, 50 mM $MgCl_2$, 50 μM $AlCl_3$, and 5 μM GDP). +AMF beads were diluted with 200 μL of assay buffer that contained AMF and were incubated for 10 min at room temperature (RT) to form the stable $G\alpha_o$–GDP–AlF_4^- complex, which RGS binds with high affinity.[30] The beads designated –AMF received 200 μL assay buffer without AMF. Then, 15 μL of RGS17–anti-GST beads was added to 96 wells of a 384-well plate. Half of these wells received $G\alpha_o$–biotin–streptavidin beads with AMF, and half received $G\alpha_o$–biotin–streptavidin beads without AMF. Half of each set of assay wells received 1 μL DMSO, which allowed us to assess the conditions of +AMF, +DMSO; +AMF, –DMSO; –AMF, +DMSO; and –AMF, –DMSO. The plate was then incubated at 4 °C in the dark for 40 min and read on a Synergy2 plate reader (BioTek, Wisnooski, VT) with a sensitivity setting of 200, excitation at 680 nM, and emission read at 570 nM.

Z factor calculation

Experiments were performed in Corning (Corning, New York, NY) 384-well white flat-bottom plates, and samples were read on a BioTek Synergy 2 plate reader. All data were collected using Gen5 (BioTek) and analyzed with GraphPad Prism 5.0 (GraphPad Software, San Diego, CA).

The 384-well plates were used to determine the positive and negative control values for the protein interaction assay. In total, 192 wells of the plate were –AMF and represented no protein–protein interaction (background), and 192 wells contained +AMF, which supports the high-affinity protein–protein interaction (maximal signal). In total, 105 μg (21 μL) of anti-GST acceptor beads and 105 μg (21 μL) streptavidin donor beads were coupled to RGS17–anti-GST and $G\alpha_o$–biotin–streptavidin at a 30nM concentration in 2.625 mL of assay buffer. The protein/bead mixtures were incubated in the dark at 4 °C for 30 min. Upon completion of coupling, the RGS17–anti-GST beads were resuspended in a total of 7.875 mL of assay buffer. The $G\alpha_o$–biotin–streptavidin bead mixture was split into two tubes of 1.312 mL each. One tube was combined with 2.625 mL of assay buffer without AMF or GDP for the no-binding control (-AMF). For the positive binding control, the second tube received assay buffer and a final concentration of 50 mM NaF, 50 mM $MgCl_2$, 50 μM $AlCl_3$,

Downloaded from jbx.sagepub.com at Novartis Global on October 21, 2011

and 5 μM GDP (+AMF) and was incubated on ice for 10 min. Then, 15 μL of RGS17–anti-GST beads was added to each well of a 384-well plate. In total, 192 wells received 15 μL of $G\alpha_o$–biotin–streptavidin beads with AMF and 192 wells received 15 μL of $G\alpha_o$–biotin–streptavidin beads without AMF using a Labsystems Multidrop dispenser (Thermo Scientific). Plates were incubated in the dark on ice for 30 min and read at RT using a Synergy 2 plate reader (BioTek) with a sensitivity setting of 200 using the AlphaScreen protocol with excitation at 680 nM and emission at 570 nM.

Z factor was calculated using the following equation: $\text{Z-factor} = 1 - \frac{3\times(\sigma p + \sigma n)}{|\mu p - \mu n|}$, where σ represents the standard deviation of positive and negative (binding and nonbinding) (*p*, *n*) controls, and μ represents the mean of positive and negative control values. Positive controls were determined using the 192 wells containing AMF and GDP, resulting in a $G\alpha_o$–RGS17 protein–protein interaction. The negative controls were determined from the 192 wells that lacked AMF and GDP, resulting in no protein–protein interaction.

Saturation binding

For saturation binding experiments, 10 nM of RGS17 was used to prepare RGS17–anti-GST beads, prepared as above using 40 μg (8 μL) of each bead to couple to each protein. Biotin–$G\alpha_o$ was serially diluted to yield a final concentration from 0.39 and 200 nM. $G\alpha_o$ protein was labeled in 33.3 μL of assay buffer containing 0.8 mL of beads and incubated for 30 min on ice. The mixture was split into equal tubes of 16.65 μL. Half of the sample received 33.35 μL of assay buffer without AMF (nonspecific binding), whereas the other half received assay buffer with 50 mM NaF, 50 mM $MgCl_2$, 50 μM $AlCl_3$, and 5 μM GDP (specific binding). The tubes were incubated in the dark on ice for 10 min. Then, 15 μL of the RGS17–anti-GST beads was added to each well. After 10 min, 15 μL of the +AMF and –AMF samples was added to their respective wells. The plate was incubated in the dark at 4 °C for 40 min and read on a Synergy 2 plate reader (BioTek) with a sensitivity setting of 150 using the AlphaScreen protocol with excitation at 680 nM and emission at 570 nM.

Competition binding

For competition binding, 10 nM of RGS17 was used to prepare RGS17–anti-GST as previously described using 10.8 μg (2.15 μL) of beads to couple the protein to the beads. $G\alpha_o$–biotin–streptavidin beads were prepared to yield a final concentration of 35 nM. A sample of 20 μL of $G\alpha_o$–biotin–streptavidin beads was removed and used as the negative control (-AMF). Half-log dilutions of free $G\alpha_o$ were plated to yield a final concentration from 1 μM to 3.16 pM. Then, 15 μL of RGS17–anti-GST beads was added to each well, to which 15 μL $G\alpha_o$–biotin–streptavidin beads was then added. Negative controls were determined in the absence of free $G\alpha_o$ and AMF, which represents background. The positive control contained AMF without free $G\alpha_o$ to define maximal binding. Plates were incubated 45 min at 4 °C and read on a Synergy 2 plate reader (BioTek) with a sensitivity setting of 200 using the AlphaScreen protocol with excitation at 680 nM and emission at 570 nM.

AlphaScreen HTS

In total, 1364 compounds from the NCI Diversity Set II were screened at a concentration of 33 μM. RGS17–anti-GST and $G\alpha_o$–biotin–streptavidin beads were prepared as previously described. In brief, 100 μg (20 μL) of beads were coupled to 20 ng (10 nM) of each binding partner ($G\alpha_o$–RGS17) and incubated for 30 min on ice. The 384-well plates containing 352 compounds and 32 wells of DMSO controls were used. Then, 15 μL of RGS17–anti-GST beads were added using a Labsystems Multidrop (Thermo Scientific) and incubated for 10 min while the $G\alpha_o$–biotin–streptavidin beads were incubated with AMF. After incubation, 15 μL of $G\alpha_o$–biotin–streptavidin beads were added to compound containing wells and incubated on ice for 30 min and read on a Synergy 2 plate reader (BioTek) with a sensitivity setting of 200 using the AlphaScreen protocol with excitation at 680 nM and emission at 570 nM.

Dose–response experiments

Experiments were carried out similarly to the high-throughput AlphaScreen assay except the final total assay volume was 60 μL, with 20 μL of $G\alpha_o$–biotin–streptavidin and RGS17–anti-GST beads at a final concentration of 10 nM. Then, 20 μL of compounds in a log dilution series to yield a final range from 1nM to 100uM was added to RGS17–anti-GST beads and incubated for 10 min in the dark on ice. Next, 20 μL of $G\alpha_o$–biotin–streptavidin beads was then added in the presence of AMF and GDP. Negative controls were determined in the absence of AMF and compound. Maximum binding was determined in the absence of compounds but in the presence of AMF and GDP.

AlphaScreen biotinlyated GST control

Compounds that inhibited the protein–protein interaction with an IC_{50} <10 μM were counterscreened in a control assay containing biotinlyated GST. Biotin–GST binds both the anti-GST and streptavidin-coated beads, bringing the beads together artificially and forcing an interaction. Compounds were diluted to yield a range from 1pM to 10uM, and 20 μL was added to each well. In 5.28 mL of assay buffer, 211 ng (42.24 μL) of anti-GST beads was incubated with 300 ρM biotin–GST for 30 min at RT. Then, 211 ng (42.24 μL) of streptavidin beads was added and incubated for 30 min on ice. After conjugation was complete, 40 μL of the anti-GST–biotin–GST–streptavidin

Downloaded from jbx.sagepub.com at Novartis Global on October 21, 2011

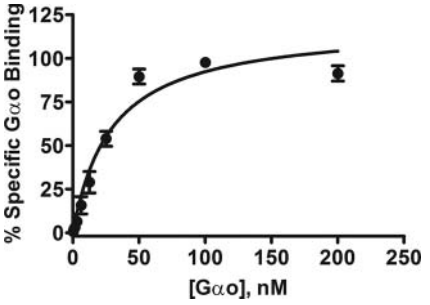

FIG. 1. Measurement of specific binding for the protein–protein interaction. Increasing concentration of biotinylated $G\alpha_o$ was added to the RGS17 on beads (10 nM; final RGS concentration) in the presence of AMF to yield the percentage of specific $G\alpha_o$ bound to RGS17. The saturation assay exhibited robust specific binding with affinity binding of 29.24 ± 4.4 nM. Nonspecific binding, determined in the absence of AMF, is less than 2% of the total binding. The graph is the average of 5 independent experiments (n = 5), performed in triplicate, with error bars indicating the standard error of the mean (SEM).

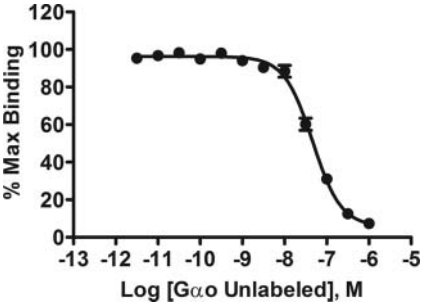

FIG. 2. Competition binding assay for $G\alpha_o$–RGS17 interaction. Increasing concentrations of un-biotinlyated $G\alpha_o$ were added to fixed concentrations of RGS17 (10 nM) and biotinlyated $G\alpha_o$ (35 nM). Competition of the free $G\alpha_o$ with the tagged G-protein yielded an IC_{50} of 46 ± 1.1 nM. The graph is the average of 4 independent experiments (n = 4), preformed in triplicate, with error bars indicating the standard error of the mean (SEM).

bead complex was added to each well of compounds, incubated for 10 min, and read at RT at a sensitivity setting of 200 on a Synergy 2 plate reader (BioTek) using the AlphaScreen protocol with excitation at 680 nM and emission at 570 nM.

RESULTS

DMSO tolerance

We tested the stability of our assay at 3.3% DMSO, our maximum conceived concentration for follow-up dose–response experiments. Our actual DMSO concentration for the HTS portion of this study was <1.5%. Under these conditions $G\alpha_o$–RGS17 screening was completed without DMSO interfering with the beads or functionality of the proteins. The +AMF, +DMSO resulted in a nonsignificant loss of signal when compared to the positive control of +AMF, –DMSO. As expected, the –AMF with and without DMSO resulted in a negligible background signal.

Affinity of RGS17 for $G\alpha_o$

We determined the affinity of RGS17 for $G\alpha_o$ using AlphaScreen. Nonspecific binding was determined using $G\alpha_o$–biotin–streptavidin beads without AMF, which was subtracted from total binding to yield specific binding. Nonspecific binding was less than 2% of total binding. **Figure 1** depicts the saturation isotherm of specific binding of the RGS17 protein with $G\alpha_o$. RGS17 (10 nM) exhibited high affinity for $G\alpha_o$ (0–200 nM) with a K_d of 29.2 ± 4.4 nM (n = 5, in triplicate). The protein–protein interaction of RGS17 and $G\alpha_o$ on beads was shown to be reversible by using free $G\alpha_o$ as a competitor, yielding an IC_{50} of 46 ± 1.1 nM and a Hill slope of –1.3 (**Fig. 2**; n = 4, in triplicate).

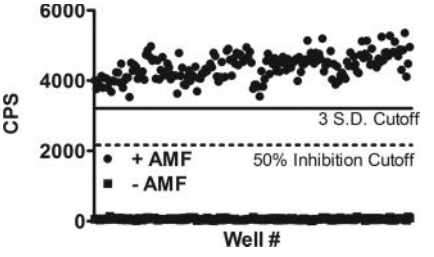

FIG. 3. Determination of the Z factor accessing the suitability of the assay for high-throughput screening. In a 384-well plate, 192 wells were used as a positive control (+AMF) and 192 wells were deprived of guanosine diphosphate (GDP) and AMF and represented negative controls. The high signal-to-noise ratio (73), coupled with the Z factor of 0.73, allows for a large screening window for compounds that inhibit the protein–protein interaction greater than 50%. A mild interplate effect was observed during the screen based on the time for reading one plate of 20 min and the proteins coming to equilibrium of the protein–protein interaction during the incubation. CPS, counts per second.

Z factor determination

One hundred ninety-two wells of a 384-well plate were used for positive controls in the presence of AMF, which affords the high-affinity $G\alpha_o$–RGS17 complex, and 192 wells were used as negative controls without AMF (**Fig. 3**). The Z factor was determined to be 0.73 with a signal-to-noise ratio of 73. This Z factor is well above the threshold 0.5 value, indicating a screening paradigm suitable for HTS.[34]

High-throughput screen for RGS17 inhibitors

This high-throughput screen focused on identifying compounds that function as inhibitors of the $G\alpha_o$–RGS17 protein–protein interaction in the presence of 50 mM NaF, 50 mM $MgCl_2$, and 50 μM $AlCl_3$ with 5 μM GDP. We interrogated the

Downloaded from jbx.sagepub.com at Novartis Global on October 21, 2011

Table 1. High-Throughput Screening Results

Initial National Cancer Institute (NCI) library, No.	1364
Primary hits (>50% inhibition), No. (%)	35 (2.5)
Confirmed hits (DRC w/RGS17), No. (%)	16 (1.17)
Inhibition of >50% versus biotin–GST control, No. (%)	4 (0.29)
IC_{50} <6 μM, No. (%)	4 (0.29)

Results of the high-throughput screening assay of the NCI Diversity Set II. Of 1364 compounds, 35 were initial hits (>50% inhibition). Primary hits were reconfirmed with a dose–response assay, and 16 compounds resulted in IC_{50} values <10 μM. GST, glutathione-S-transferase.

Table 2. Summary of DRC from Initial Hits

Compounds	*% Inhibition of Biotin–GST Control at 10 μM*	*% Inhibition of RGS17–Gα$_o$ Control at 10 μM*	*IC_{50} for Biotin–GST*	*IC_{50} for RGS17–Gα$_o$*
RL-1	14.3	80.7	1.40 μM	1.40 μM
RL-2	15.9	74.5	10.00 μM	2.40 μM
RL-3	41.5	89.8	727 M	0.620 μM
RL-4	21.2	74.2	12.00 μM	5.40 μM
RL-5	50.1	75.0	0.004 M	8.40 μM
RL-6	30.8	75.0	31.00 μM	23.60 μM
RL-7	45.2	75.0	0.003 M	4.10 μM
RL-8	35.0	63.4	1.90 M	5.00 μM
RL-9	64.3	91.8	22.00 μM	0.800 μM
RL-10	59.8	67.0	0.021 M	15.00 μM
RL-11	53.3	64.4	0.052 M	3.00 μM
RL-12	51.9	75.7	0.120 M	3.40 μM
RL-13	73.0	80.7	1.40 μM	2.70 μM
RL-14	57.3	80.5	2.38 M	0.17 μM
RL-15	32.0	63.5	3.20 M	2.80 μM
RL-16	66.9	63.1	0.86 μM	2.20 μM

Compounds screened against the biotin–GST control resulted in four compounds exhibiting ≥50% inhibition of the Gα$_o$–RGS17 interaction at a compound concentration of 10 μM when compared to the screen against the biotin–GST control at 10 μM. All four compounds exhibited IC_{50} values <6 μM. The activity against the Gα$_o$–RGS17 dose–response curves was held to a standard of ≥50% inhibition against the control. The four compounds RL-1, RL-2, RL-3, and RL-4 were found to have activity in the biotin–GST control as shown by favorable IC_{50}s but were chosen for their activity of inhibition at 10-μM concentrations.

NCI Diversity Set II, which consisted of 1364 compounds. RGS17 and activated Gα$_o$, coupled to their respective beads and in the presence of compounds at 33 μM, were read on the Synergy 2 plate reader (BioTek) at a sensitivity setting of 200. We used a cutoff of 50% inhibition or greater to consider an initial hit. We observed a 2.5% initial hit frequency (35 compounds) with 16 of those compounds confirmed with dose–response curves to exhibit an IC_{50} <10 μM (**Table 1**), yielding a confirmed hit rate of 1.17%. These 16 compounds were then subjected to a counterscreen against the biotinylated GST control to eliminate compounds that interfere with the AlphaScreen assay itself. **Table 2** shows the effect of the compounds on the Gα$_o$–RGS17 protein–protein interaction as compared to their effect on the AlphaScreen assay reagents themselves using biotin–GST. Twelve of the 16 compounds showed minimal activity in the counterscreen. Four compounds were found to inhibit the Gα$_o$–RGS17 protein–protein interaction greater than

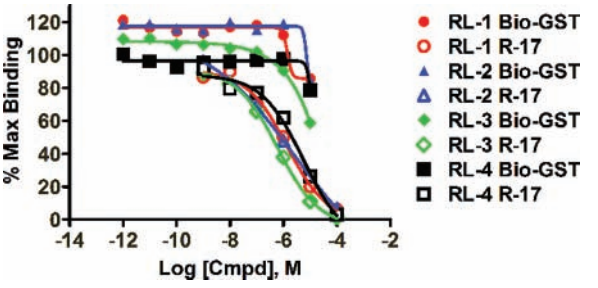

FIG. 4. Dose–response curves for the four compounds using AlphaScreen. RGS17–GST fusion protein (10 nM) and biotinylated Gα$_o$ (10 nM) were coupled to their respective beads. RGS17 beads were preincubated with increasing concentrations of compound before addition of 5 nM AMF-activated Gα$_o$ beads. All four exhibited Gα$_o$–RGS17 protein–protein interaction with IC_{50} values of 1.4 μM (RL-1), 2.4 μM (RL-2), 0.62 μM (RL-3), and 5.4 μM (RL-4). Error bars indicate the standard error of the mean (SEM).

50% at 10 μM (**Fig. 4**). The >50% inhibition was determined by comparison of the dose response and counterscreen and resulted in a confirmed hit rate of 0.29%, as well as four new compounds identified as inhibitors of the Gα$_o$–RGS17 protein–protein interaction. These four compounds were subjected to a counterscreen for activity using FCPIA, which yielded two confirmed lead compounds.

DISCUSSION

RGS proteins continue to emerge as attractive targets to exploit to modulate GPCR signaling.[6,35–38] Recent years have seen the establishment and advance of HTS for inhibitors of RGS proteins. Early work used yeast-based screening for inhibitors of RGS4, which were fully automated and performed in a 384-well format.[39] The first structure of a small-molecule RGS inhibitor was described for RGS4 by Roman et al.[30] These studies provided the proof of principle that small molecules could modulate the action of RGS proteins. Our study focused on the Gα$_o$–RGS17 protein interaction with the aim of simplifying the assay and increasing the throughput by which we could interrogate small-molecule libraries while maintaining a robust Z factor and excellent signal-to-noise ratio. With this novel screening assay, we were able to achieve both of these goals while reducing the amount of expensive protein and reagents.

To establish the most suitable screening parameters for this AlphaScreen assay, we first fully characterized the binding characteristics of the purified Gα$_o$ subunit and RGS17, with the Gα$_o$ subunit in its high-affinity state induced by GDP and AlF_4^{-30}, which binds stably to RGS proteins. Sternweis et al.[40] showed that activation of the Gα subunit by the introduction of AMF into the buffer produced an affinity state that mimicked the physiological affinity of the protein–protein interaction. Our strategy

Downloaded from jbx.sagepub.com at Novartis Global on October 21, 2011

for detection of the protein–protein interaction is depicted in **Supplemental Figure S1**. RGS17 was purified from *Escherichia coli* as an N-terminal-GST fusion protein and bound to anti-GST-coated acceptor beads. $G\alpha_o$ purified from *E. coli* as previously described[32,33,41] was chemically biotinylated using maleimide chemistry and subsequently bound to streptavidin-coated donor beads. A protein–protein interaction is detected between the binding partners via the donor acceptor beads when they are brought within 200 nm of each other. Mechanistically, singlet oxygen, O_2 ($a^1\Delta_g$), is released from the donor bead upon excitement at 680 nm. In its short lifetime (<3 μs), the singlet oxygen species can travel up to 200 nm to reach an acceptor bead and induce a chemiluminescent reaction within the acceptor bead that results in photon emission that can be detected at 570 nm.

First, we demonstrated that the $G\alpha_o$–RGS17 protein interaction could accurately be detected and quantitated (**Figs. 1**–**3**). The saturation study also allowed for the determination of the relative K_d value for the $G\alpha_o$–RGS17 interaction to be 29 ± 4.4 nM. The determined K_d value for RGS17 compared very favorably to the K_d determined by FCPIA screens for other RGS proteins in both multiplex and singlet for RGS4 (115 ± 6 and 91 ± 9 nM), RGS8 (23 ± 2 and 24 ± 2 nM), RGS16 (54 ± 7 and 37 ± 6 nM), RGS6 (478 ± 27 and 340 ± 52 nM), and RGS7 (63 ± 2 and 72 ± 5 nM).[32] Second, the competition binding experiment results demonstrate that we could displace the biotin–$G\alpha_o$ with untagged $G\alpha_o$ with an IC_{50} value of 46 ± 1.1 nM. This was important as it demonstrates the reversibility of the $G\alpha_o$–RGS17 interaction even in the high-affinity binding state afforded by AMF and GDP. These experiments guided us in choosing a screening concentration of 10 nM for $G\alpha_o$ that was within the linear portion of the saturation curve and would provide sensitive detection of inhibitors.

In our screen, we identified 35 compounds as primary hits for an initial hit rate of 2.5%, and we further filtered those hits by dose–response curves and confirmed 16 compounds with IC_{50} values less than 10 μM, for a confirmation rate of 1.17%. We then screened these 16 compounds against a biotinlyated GST control that artificially brings donor and acceptor beads together. Any inhibition of the signal by a compound would indicate a nonspecific action of that compound on the AlphaScreen assay itself. This powerful and convenient control screen was done to eliminate compounds that could possibly inhibit the AlphaScreen signal. Potential reasons for inhibition could be from O_2 quenchers, absorbance at the excitation wavelength for our donor beads (680 nM), interference with the anti-GST antibody used to conjugate the RGS17–GST fusion protein to the donor bead, or interference with the chemiluminescent reaction within the bead. The possibility of compound aggregates as a potential reason for signal inhibition was eliminated by the addition of detergent in the assay buffer, which has been shown to suppress the nonspecific effects of aggregates in HTS.[42] Following controls, we identified four novel compounds that acted to specifically inhibit the $G\alpha_o$–RGS17 interaction. These four compounds that were confirmed to inhibit the RGS17–$G\alpha_o$ protein–protein interactions greater than 50% over the biotinylated GST control were counterscreened for activity using FCPIA.[30,32] Compounds RL-1 and RL-2 exhibited strong concentration dependence that correlated with AlphaScreen results (IC_{50} ~10 μM), whereas compounds RL-3 and RL-4 did not inhibit the RGS17–$G\alpha_o$ protein–protein interaction. These compounds will be further tested for functional activity in a steady-state GTPase assay to investigate the mechanism of action in blocking the protein–protein interaction.

One of the major advancements in this study is the discovery of the first small-molecule inhibitors for the $G\alpha_o$–RGS17 protein–protein interaction. These inhibitors exhibit potencies that are less than 6 μM. Further studies and structural optimization to establish activity in cells and specificity for this protein–protein interaction are being undertaken by our lab with the hopes of establishing the first RGS17 inhibitor to work in whole cells. Optimization of the structure may be necessary to develop a molecule that is cell permeable. Nevertheless, our findings add to the now growing literature of small-molecule RGS inhibitors and represent a novel HTS assay in a 384-well format that can be adapted for use with other RGS proteins and their binding partners.

The second advancement of this study is the increase in the number of compounds that can be screened without a decrease in the robustness of the assay. One of the current methods used in screening for small-molecule inhibitors is the FCPIA approach. This is done using 96-well plates and methods described in Roman et al.[30,32] Another method that has been applied to HTS is time-resolved fluorescence resonance energy transfer (TR-FRET), which has been used to identify the first small-molecule inhibitors of an RGS protein that exhibited activity in cells and was completed in a 384-well format.[41] The AlphaScreen resulted in an initial hit rate of 2.5% of 1300 compounds in the primary screen, with a DRC confirmation rate of 1.17% and filtered results for an overall hit rate 0.29%. This compares favorably with the polyplexed FCPIA screen for inhibitors of multiple RGS protein interactions[32] (initial hit rate, 1.5%–3.9%; filtered results, 0.3%–1.4%; and overall hit rate of 0.375%). The AlphaScreen exhibited a high initial hit rate when compared to the TR-FRET screen's initial hit rate of 0.37% but was well within the overall expected hit rate.[41] Our approach represents a novel screening paradigm that increases throughput while maintaining a very robust Z factor and signal-to-noise ratio. Furthermore, our screen allowed us to screen three 384-well plates per hour, resulting in 1056 compounds screened in 1 h. One limitation of the throughput in this study is the speed of the plate reader; other readers, such as the EnVision from PerkinElmer can read 384-well plates in less than 2 min, which would allow this assay's throughput to be increased manifold. This AlphaScreen assay format should

Downloaded from jbx.sagepub.com at Novartis Global on October 21, 2011

prove powerful, as it could be readily adapted to many RGS protein interactions.

In this report, we focus on RGS17 as a novel target for discovery of potential novel anticancer agents. Recent fine mapping studies of chromosome 6q23-25 have revealed the *RGS17* gene as a likely candidate gene in cases of familial lung cancer,[16] and RGS17 has been shown as an overexpressed gene in human lung and prostate cancers, leading to the induction of cell proliferation and the control of tumor load in nude mice.[15,16] Effective RNAi knockdown studies have shown that tumor burden and proliferation can be significantly reduced in cell culture and nude mice models injected with H1299 cells (non-small-cell lung carcinoma cell line) that have been subjected to RGS17 knockdown by RNAi.[15,16] Therefore, the development of a small-molecule inhibitor that could act on RGS17 in a similar way as the RNAi knockdown experiments presents another therapeutic approach for cancer treatment for this novel application of the AlphaScreen technology for usage in HTS.

In conclusion, we demonstrated that the AlphaScreen technology could be adapted to allow for the interrogation of small-molecule chemical libraries yielding the first inhibitors of specific protein–protein interactions involving RGS17 and $G\alpha_o$. In addition, our method, using GST-fusion proteins for purification and bead coupling, greatly simplifies the preparation of material for the screen. This method is also powerful in that it can be adapted for many RGS proteins and their cognate G-protein alpha subunits. This study presents a method that can increase the number of compounds screened and provides another target for using AlphaScreen as a method of HTS for inhibitors of protein–protein interactions.

ACKNOWLEDGMENTS

This work was supported by an American Cancer Society Seed Grant through the University of Iowa Holden Comprehensive Cancer Center's ACS Institutional Research Grant IRG-77-004-31. The authors acknowledge the NCI/DTP Open Chemical Repository (http://dtp.cancer.gov) for providing the chemical library used in this work.

REFERENCES

1. Pierce, K. L.; Premont, R. T.; Lefkowitz, R. J. Seven-Transmembrane Receptors. *Nat. Rev. Mol. Cell. Biol.* **2002**, *3*, 639–650.
2. Dorsam, R. T.; Gutkind, J. S. G-Protein-Coupled Receptors and Cancer. *Nat. Rev. Cancer* **2007**, *7*, 79–94.
3. Gilman, A. G. G Proteins: Transducers of Receptor-Generated Signals. *Annu. Rev. Biochem.* **1987**, *56*, 615–49.
4. Ross, E. M.; Wilkie, T. M. GTPase-Activating Proteins for Heterotrimeric G Proteins: Regulators of G Protein Signaling (RGS) and RGS-Like Proteins. *Annu. Rev. Biochem.* **2000**, *69*, 795–827.
5. McCoy, K. L.; Hepler, J. R. Chapter 3 Regulators of G Protein Signaling Proteins as Central Components of G Protein-Coupled Receptor Signaling Complexes. *Prog. Mol. Biol. Transl. Sci.* **2009**, *86*, 49–74.
6. Roman, D. L. Chapter 11 Identification of Ligands Targeting RGS Proteins High-Throughput Screening and Therapeutic Potential. *Prog. Mol. Biol. Transl. Sci.* **2009**, *86*, 335–356.
7. Cho, H.; Kehrl, J. H. Chapter 9 Regulation of Immune Function by G Protein-Coupled Receptors, Trimeric G Proteins, and RGS Proteins. *Prog. Mol. Biol. Transl. Sci.* **2009**, *86*, 249–298.
8. Jemal, A.; Siegel, R.; Xu, J.; Ward, E. Cancer Statistics, 2010. *CA Cancer J. Clin.* **2010**.
9. Grunebach, F.; Erndt, S.; Häntschel, M.; Heine, A.; Brossart P. Generation of Antigen-Specific CTL Responses Using RGS1 mRNA Transfected Dendritic Cells. *Cancer Immunol. Immunother.* **2008**, *57*, 1483–1491.
10. Rangel, J.; Nosrati, M.; Leong, S. P.; Haqq, C.; Miller, J. R., III., ; Sagebiel, R. W.; Kashani-Sabet, M. Novel Role for RGS1 in Melanoma Progression. *Am. J. Surg. Pathol.* **2008**, *32*, 1207–1212.
11. Smalley, M. J.; Iravani, M.; Leao, M.; Grigoriadis, A.; Kendrick, H.; Dexter, T.; Fenwick, K.; Regan, J. L.; Britt, K.; McDonald, S.; et al. Regulator of G-protein Signalling 2 mRNA Is Differentially Expressed in Mammary Epithelial Subpopulations and Over-expressed in the Majority of Breast Cancers. *Breast Cancer Res.* **2007**, *9*, R85.
12. Boss, C. N.; Grünebach, F.; Brauer, K.; Häntschel, M.; Mirakaj, V.; Weinschenk, T.; Stevanovic, S.; Rammensee, H. G.; Brossart, P. Identification and Characterization of T-Cell Epitopes Deduced from RGS5, a Novel Broadly Expressed Tumor Antigen. *Clin Cancer Res.* **2007**, *13*, 3347–3355.
13. Hurst, J. H.; Mendpara, N.; Hooks, S. B. Regulator of G-protein Signalling Expression and Function in Ovarian Cancer Cell Lines. *Cell. Mol. Biol. Lett.* **2009**, *14*, 153–174.
14. Riker, A. I.; Enkemann, S. A.; Fodstad, O.; Liu, S.; Ren, S.; Morris, C.; Xi, Y.; Howell, P.; Metge, B.; Samant, R. S.; et al. The Gene Expression Profiles of Primary and Metastatic Melanoma Yields a Transition Point of Tumor Progression and Metastasis. *BMC Med. Genomics* **2008**, *1*, 13.
15. James, M. A.; Lu, Y.; Liu, Y.; Vikis, H. G.; You, M. RGS17, an Overexpressed Gene in Human Lung and Prostate Cancer, Induces Tumor Cell Proliferation through the Cyclic AMP-PKA-CREB Pathway. *Cancer Res.* **2009**, *69*, 2108–2116.
16. You, M.; Wang, D.; Liu, P.; Vikis, H.; James, M.; Lu, Y.; Wang, Y.; Chen, Q.; Jia, D.; Liu, Y., et al. Fine Mapping of Chromosome 6q23-25 Region in Familial Lung Cancer Families Reveals RGS17 as a Likely Candidate Gene. *Clin. Cancer Res.* **2009**, *15*, 2666–2674.
17. Larminie, C.; Murdock, P.; Walhin, J. P.; Duckworth, M.; Blumer, K. J.; Scheideler, M. A.; Garnier, M. Selective Expression of Regulators of G-Protein Signaling (RGS) in the Human Central Nervous System. *Brain Res. Mol. Brain Res.* **2004**, *122*, 24–34.
18. Mao, H.; Zhao, Q.; Daigle, M.; Ghahremani, M. H.; Chidiac, P.; Albert, P. R. RGS17/RGSZ2, a Novel Regulator of Gi/o, Gz, and Gq Signaling. *J. Biol. Chem.* **2004**, *279*, 26314–2622.
19. Technikova-Dobrova, Z.; Sardanelli, A. M.; Speranza, F.; Scacco, S.; Signorile, A.; Lorusso, V.; Papa, S. Cyclic Adenosine Monophosphate-Dependent Phosphorylation of Mammalian Mitochondrial Proteins: Enzyme and Substrate Characterization and Functional Role. *Biochemistry* **2001**, *40*, 13941–13947.
20. Kim, C.; Vigil, D.; Anand, G.; Taylor, S. S. Structure and Dynamics of PKA Signaling Proteins. *Eur. J. Cell Biol.* **2006**, *85*, 651–654.
21. Taylor, S. S.; Kim, C.; Vigil, D.; Haste, N. M.; Yang, J.; Wu, J.; Anand, G. S. Dynamics of Signaling by PKA. *Biochim. Biophys. Acta* **2005**, *1754*, 25–37.
22. Shaywitz, A. J.; Greenberg, M. E. CREB: A Stimulus-Induced Transcription Factor Activated by a Diverse Array of Extracellular Signals. *Annu. Rev. Biochem.* **1999**, *68*, 821–861.

Downloaded from jbx.sagepub.com at Novartis Global on October 21, 2011

23. Mayr, B.; Montminy, M. Transcriptional Regulation by the Phosphorylation-Dependent Factor CREB. *Nat. Rev. Mol. Cell. Biol.* **2001**, *2*, 599–609.
24. Lonze, B. E.; Ginty, D. D. Function and Regulation of CREB Family Transcription Factors in the Nervous System. *Neuron* **2002**, *35*, 605–623.
25. Choi, Y. J.; Kim, S. Y.; Oh, J. M.; Juhnn, Y. S. Stimulatory Heterotrimeric G Protein Augments Gamma Ray–Induced Apoptosis by Up-regulation of Bak Expression via CREB and AP-1 in H1299 Human Lung Cancer Cells. *Exp. Mol. Med.* **2009**, *41*, 592–600.
26. Rosenberg, D.; Groussin, L.; Jullian, E.; Perlemoine, K.; Bertagna, X.; Bertherat, J. Role of the PKA-Regulated Transcription Factor CREB in Development and Tumorigenesis of Endocrine Tissues. *Ann. N. Y. Acad. Sci.* **2002**, *968*, 65–74.
27. Cekanova, M.; Majidy, M.; Masi, T.; Al-Wadei, H. A.; Schuller, H. M. Overexpressed Raf-1 and Phosphorylated Cyclic Adenosine 3′-5′-Monophosphatate Response Element-Binding Protein Are Early Markers for Lung Adenocarcinoma. *Cancer* **2007**, *109*, 1164–1173.
28. Uehara, Y.; Mochizuki, M.; Matsuno, K.; Haino, T.; Asai, A. Novel High-Throughput Screening System for Identifying STAT3-SH2 Antagonists. *Biochem. Biophys. Res. Commun.* **2009**, *380*, 627–631.
29. Yi, F.; Zhu, P.; Southall, N.; Inglese, J.; Austin, C. P.; Zheng, W.; Regan, L. An AlphaScreen-Based High-Throughput Screen to Identify Inhibitors of Hsp90-Cochaperone Interaction. *J. Biomol. Screen.* **2009**, *14*, 273–281.
30. Roman, D. L.; Talbot, J. N.; Roof, R. A.; Sunahara, R. K.; Traynor, J. R.; Neubig, R. R. Identification of Small-Molecule Inhibitors of RGS4 Using a High-Throughput Flow Cytometry Protein Interaction Assay. *Mol. Pharmacol.* **2007**, *71*, 169–175.
31. Roof, R. A.; Sobczyk-Kojiro, K.; Turbiak, A. J.; Roman, D. L.; Pogozheva, I. D.; Blazer, L. L.; Neubig, R. R.; Mosberg, H. I. Novel Peptide Ligands of RGS4 from a Focused One-Bead, One-Compound Library. *Chem. Biol. Drug Des.* **2008**, *72*, 111–119.
32. Roman, D. L.; Ota, S.; Neubig, R. R. Polyplexed Flow Cytometry Protein Interaction Assay: A Novel High-Throughput Screening Paradigm for RGS Protein Inhibitors. *J. Biomol. Screen.* **2009**, *14*, 610–619.
33. Lee, E.; Linder, M. E.; Gilman, A. G. Expression of G-Protein Alpha Subunits in *Escherichia coli*. *Methods Enzymol.* **1994**, *237*, 146–164.
34. Zhang, J. H.; Chung, T. D.; Oldenburg, K. R. A Simple Statistical Parameter for Use in Evaluation and Validation of High Throughput Screening Assays. *J. Biomol. Screen.* **1999**, *4*, 67–73.
35. Neubig, R. R. Regulators of G Protein Signaling (RGS Proteins): Novel Central Nervous System Drug Targets. *J. Pept. Res.* **2002**, *60*, 312–316.
36. Neubig, R. R.; Siderovski, D. P. Regulators of G-Protein Signalling as New Central Nervous System Drug Targets. *Nat. Rev. Drug Discov.* **2002**, *1*, 187–197.
37. Zhong, H.; Neubig, R. R. Regulator of G Protein Signaling Proteins: Novel Multifunctional Drug Targets. *J. Pharmacol. Exp. Ther.* **2001**, *297*, 837–845.
38. Sjogren, B.; Neubig, R. R. Thinking Outside of the "RGS box": New Approaches To Therapeutic Targeting of Regulators of G Protein Signaling. *Mol. Pharmacol.* **2010**, *78*, 550–557.
39. Young, K. H.; Wang, Y.; Bender, C.; Ajit, S.; Ramirez, F.; Gilbert, A.; Nieuwenhuijsen, B. W. Yeast-Based Screening for Inhibitors of RGS Proteins. *Methods Enzymol.* **2004**, *389*, 277–301.
40. Sternweis, P. C.; Northup, J. K.; Smigel, M. D.; Gilman, A. G. The Regulatory Component of Adenylate Cyclase: Purification and Properties. *J. Biol. Chem.* **1981**, *256*, 11517–11526.
41. Blazer, L. L.; Roman, D. L.; Chung, A.; Larsen, M. J.; Greedy, B. M.; Husbands, S. M.; Neubig, R. R. Reversible, Allosteric Small-Molecule Inhibitors of Regulator of G Protein Signaling Proteins. *Mol. Pharmacol.* **2010**, *78*, 524–533.
42. Shoichet, B. K. Screening in a Spirit Haunted World. *Drug Discov. Today* **2006**, *11*, 607–615.

Address correspondence to:
David L. Roman
Department of Pharmaceutical Sciences
and Experimental Therapeutics
Division of Medicinal and Natural Products Chemistry
College of Pharmacy, University of Iowa
115 South Grand Avenue, Iowa City, IA 52242

E-mail: david-roman@uiowa.edu

Downloaded from jbx.sagepub.com at Novartis Global on October 21, 2011